PAPER • OPEN ACCESS

Analysis crystal structure of magnetic materials $Co_{1-x}Zn_xFe_2O_4$

View the article online for updates and enhancements.

IOP ebooks™

Bringing you innovative digital publishing with leading voices to create your essential collection of books in STEM research.

Start exploring the collection - download the first chapter of every title for free.

Analysis crystal structure of magnetic materials $Co_{1-x}Zn_xFe_2O_4$

Akmal Johan[1,2a], Wisnu Ari Adi[3], Fitri Suryani Arsyad[1] and Dedi Setiabudidaya[1]

[1] Department of Physics, Faculty of Mathematics and Natural Science, Sriwijaya University, Indralaya South Sumatra 30862, Indonesia
[2] Graduate School of Sciences, Faculty of Mathematics and Natural Sciences, Sriwijaya University, Indonesia;
[3] Centre for Science and Technology of Advanced Materials, National Nuclear Energy Agency of Indonesia, Kawasan Puspiptek Serpong, Tangerang Selatan 15314, Indonesia

Email: [a] akmal_johan@mipa.unsri.ac.id

Abstract. Modification of zinc substitution cobalt ferrite material is expected to be one of the microwave absorbing material candidates because it has single phase permittivity and permeability. Permitivity and permeability are engineered from the inter-substitution of atoms in the crystal lattice as a function of composition. Substitution of zinc into cobalt ferrite ($Co_{1-x}Zn_xFe_2O_4$) for Zn^{2+} (x = 0 − 1) has been synthesized using the solid reaction method through mechanical deformation techniques. The results of refinement of X-ray diffraction patterns indicates that a single phase is obtained for all x compositions. Cubic structure formation with Fd3m space group, where the lattice parameter, lattice strain, cell unit volume, and atomic density change as a composition function. Morphological observations of particles using a scanning electron microscope showed that the particle size distribution was evenly distributed for all compositions with particle sizes ranging from 100-500 nm, whereas in each particle the average size of crystallite also changed as a function of composition. It was concluded that the effect of Zn substitution on $Co_{1-x}Zn_xFe_2O_4$ resulted in changes in the crystal structure parameters as a function of composition with a uniform particle size distribution in all compositions.

1. Introduction

Lately, technological developments, especially in electronics and telecommunications, especially cellular phones (cellphones) are increasing sharply. cellphones with electronic components that work at high frequencies often experience frequency leakage. This phenomenon is called EMI (electromagnetic wave interference). EMI phenomenon can interfere with the performance of the electronic component itself. Therefore, an electromagnetic wave absorbent (absorber) is needed to avoid frequency leakage [1-3]. The requirements that must be met by a material to be used as an absorbent material for electromagnetic waves is that the material must have both permeability, permittivity, resistivity and high magnetic saturation, but it has a low coercivity field, so the reflection loss value generated by the material is sufficient big [4-6]. One example of absorber material that is widely developed today is spinel-ferrite based magnetic material which has a very high permeability value [7-10].

The development of ferrite spinel-based magnetic materials has attracted the attention of many researchers and industry players in view of its wide application, especially in the electronics and telecommunications industries. This is based on the ferrite spinel-based magnetic material to date still dominates the world market share. For researchers, the ferrite spinel compound is attractive because of its promising magnetism to be explored further in connection with the physical phenomena that arise, including its potential to become a microwave absorbent material, because its permeability as a high-frequency function is mainly used in frequency regions microwaves [11-12]. The advantages of ferrite magnetic compounds include addition of its main components based on iron oxide (Fe_2O_3) which is abundant in availability and can be produced at relatively inexpensive, easy and simple costs with a less difficult method such as solid state reaction [13-14], and sol gel [15]. This type of magnetic material has oxide phases which are built on very strong ionic bonds. This shows that in general atmospheric conditions, these compounds are chemically and physically very stable.

This research will explore the absorption properties of microwaves from cobalt ferrite ($CoFe_2O_4$) based magnetic materials. In addition, the direction of this research is also still very up-to-date, considering the use of ferrite-based magnetic material as a microwave absorbent material until it is still open to be developed. Engineering of the crystal structure will be carried out through ionic substitution by engineering materials into nanocrystalline materials through mechanical deformation techniques. $CoFe_2O_4$ is a magnetic compound that has a structure of cubic spinel crystals containing Co^{2+} and Fe^{3+} ions. Co^{2+} ions occupy a tetrahedral site, while Fe^{3+} ions occupy an octahedral site [16]. $CoFe_2O_4$ is classified as a soft magnetic material with a low coercivity field and high saturation magnetization which makes this material has a high permeability value and is very suitable for applications as microwave absorbing material. Zn^{2+} ion substitution is expected to increase the value of the permittivity of this material so as to make this material have a single permeability and permittivity value. As an initial study, the discussion will focus on the analysis of the crystal structure of cobalt ferrite based magnetic materials substituted with Zn^{2+} ions, both in terms of phase formation, changes in lattice parameters, crystallite size, lattice strains, and cationic distribution. While the magnetic properties will be seen from the changes in magnetic exchange interactions (Co-O-Fe) through the approach of calculating the bond distance between the atoms.

2. Materials and Method

The $Co_{1-x}Zn_xFe_2O_4$ system is prepared from cobalt ferrite substituted with Zn^{2+} using a solid reaction method through mechanical deformation techniques with several raw materials namely CoO (Merck, purity 99.9%), ZnO (Merck, purity 99.9%), and Fe_2O_3 (Sigma-Aldrich, purity of 99.9%). Stoichiometric calculations for each composition of Zn^{2+} are shown in Table 1.

Table 1. Stoichiometry calculation sample $Co_{1-x}Zn_xFe_2O_4$.

Composition, x	Name		Raw material mass (grams)		
	Sample	Code	CoO	ZnO	Fe_2O_3
0	$CoFe_2O_4$	CZF-0	2.5989	-	7.4011
0.25	$Co_{0.75}Zn_{0.25}Fe_2O_4$	CZF-1	1.9080	0.8473	7.2447
0.5	$Co_{0.5}Zn_{0.5}Fe_2O_4$	CZF-2	1.2457	1.6595	7.0948
0.75	$Co_{0.25}Zn_{0.75}Fe_2O_4$	CZF-3	0.6102	2.4388	6.9510
1	$ZnFe_2O_4$	CZF-4	-	3.1872	6.8128

The three raw materials are weighed according to the composition of each then mixed and milled for 5 hours in a 50 ml ethanol environment using a high energy milling device PW-1000di. The mass ratio of milling balls (diameter 10 mm) with material is 2:1. Then the milling mixture is dried in an oven at 100^oC for 4 hours. Then the sample was sintered using Thermolyne 6000 furnace at 1000^oC for 5 hours. To find out the changes in the crystal structure parameters of the material due to the influence of Zn^{2+} substitution, the samples were characterized using Pan Analytical brand X-ray diffraction equipment with CuKα X-ray anode (λ = 1.5406 Å) with step size 0.0263^o. Qualitative analysis using the Match program and quantitative analysis is carried out using the general structure analysis system

(GSAS) software and the Vesta program. While the surface morphology and particle size were observed using a scanning electron microscope (SEM) equipment brand JEOL type JED 350.

3. Results and Discussions

In Figure 1 shows X-ray diffraction (XRD) patterns results of measurement of ferrite cobalt magnetic samples of Zn^{2+} ($Co_{1-x}Zn_xFe_2O_4$) for x = 0–1 using X-ray diffractometer. The results of qualitative analysis using the Match program found that all samples were single phase spinel ferrite with cubic crystal symmetry (Fd-3m space group) [17]. The peaks of the XRD pattern for all samples strongly correspond to crystallography open database (COD: 00-043-0002). This X-ray diffraction pattern is also similar to the XRD pattern peaks in previous studies [17-18].
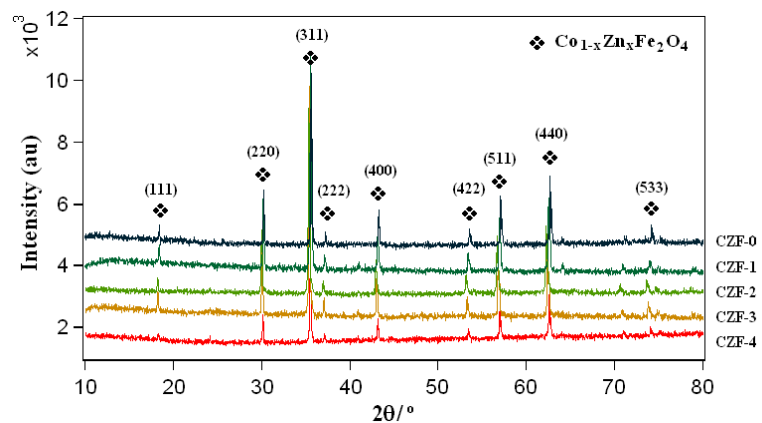

Figure 1. Qualitative analysis results of sample X-ray diffraction patterns $Co_{1-x}Zn_xFe_2O_4$ (x = 0 – 1)

The results of qualitative analysis using the Match program show that all peaks were identified as single-phase with the Miller field (111), (220), (311), (222), (400), (422), (511), (440) indexes. and (533) respectively at the angle of Bragg 18.36^o; 30.19^o; 35.54^o; 37.21^o; 43.19^o; 53.62^o; 57.08^o; 62.67^o; and 71.12^o. The result of this single phase identification is very interesting to understand because it is indicated that zinc atoms have been successfully substituted to replace some of the cobalt atoms in the structure of $CoFe_2O_4$. In Figure 1 it also appears that with the presence of Zn substitution in the sample, a peak shift occurs as shown in Figure 2.
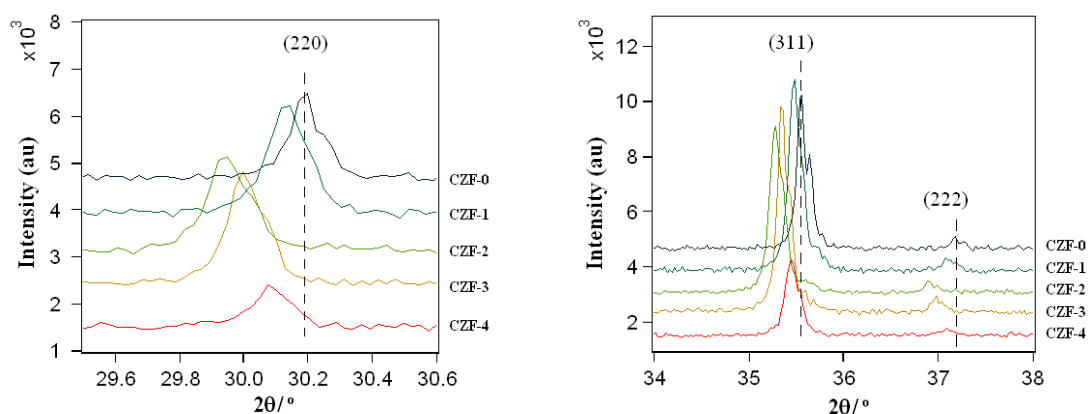

Figure 2. The peaks shift from the sample X-ray diffraction pattern $Co_{1-x}Zn_xFe_2O_4$ (x = 0 – 1)

The Bragg diffraction peaks gradually shift to the left which is lower as the Zn concentration increases proportional to Co in the cobalt ferrite lattice and shifts right again after this Zn concentration increases until a single zinc ferrite phase ($ZnFe_2O_4$) is formed. In Figure 2 it is clearly observed that the plane 220 shifts from Bragg diffraction 30.19 (CZF-0) to 30.30 (CZF-2). Similarly in fields (311) and (222) experienced successive peak shifts from Bragg diffraction 34.13 (CZF-0) to 34.23 (CZF-2) and 34.13 (CZF-0) to 34.23 (CZF-2). This is presumably because the size of the Zn^{2+} ion radius is greater (0.99 Å) than the Co^{2+} (1.49Å) ion radius. This will also have an impact on changes in the crystal structure parameters of this system material. More detailed discussion related to the effect of Zn substitution on ferrite cobalt lattice will be discussed in more detail based on the results of quantitative analysis of this XRD pattern, so further analysis is needed to determine phase formation, changes in lattice parameters, crystallite size, lattice strains, and cationic distribution of results. substitution of Zn into this cobalt ferrite lattice.

In Figure 3 shows the results of quantitative analysis of X-ray diffraction patterns from $Co_{1-x}Zn_xFe_2O_4$ samples with variations in composition (x = 0-1).

(a) x = 0

(d) x = 0.75

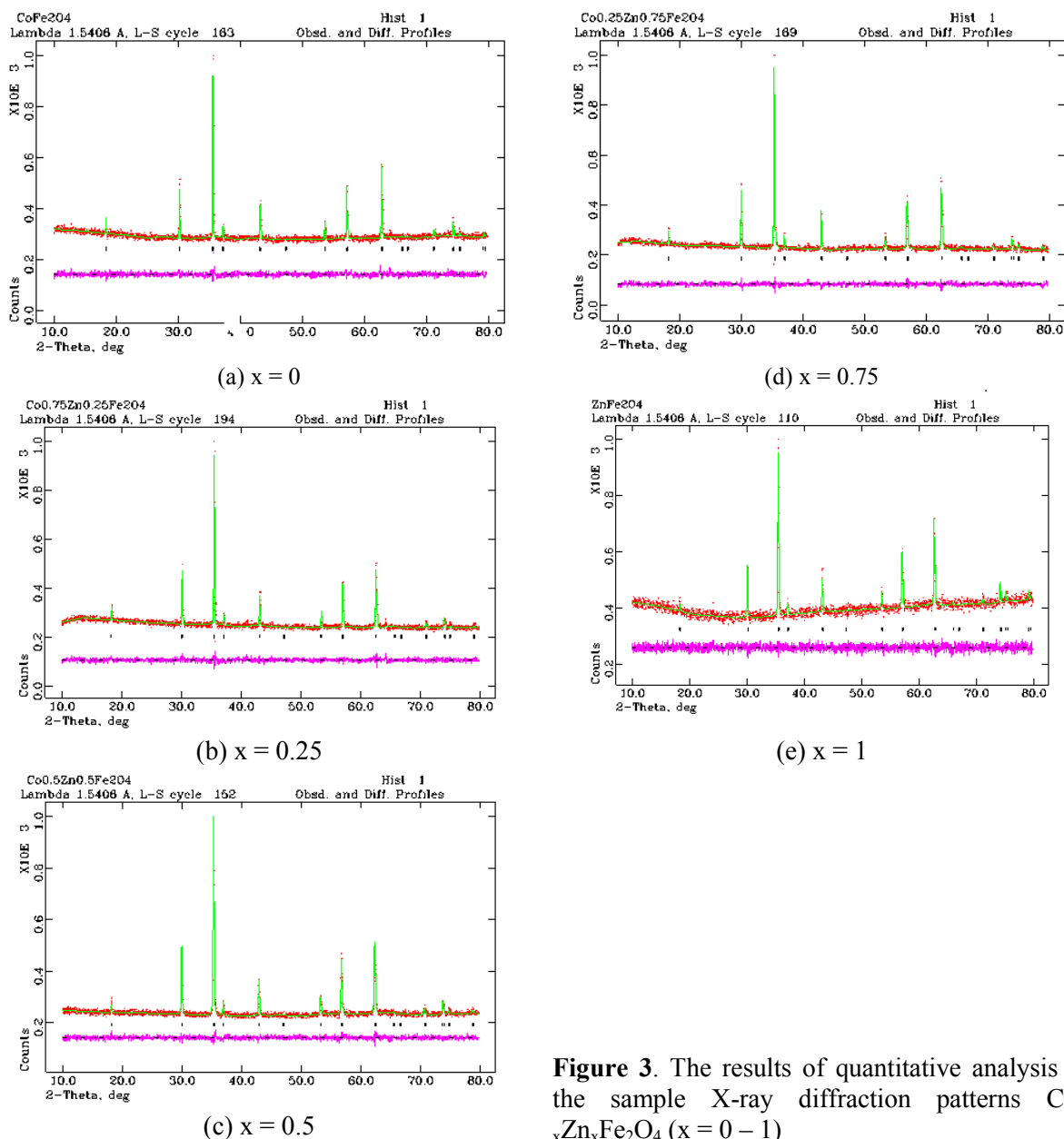

(b) x = 0.25

(e) x = 1

(c) x = 0.5

Figure 3. The results of quantitative analysis of the sample X-ray diffraction patterns $Co_{1-x}Zn_xFe_2O_4$ (x = 0 − 1)

Figure 3 (a-e) is the result of refinement of the XRD pattern for x = 0-1 which has formed a single phase bragg diffraction peak with a single phase following the spinel ferrite structure with cubic crystal symmetry (Fd-3m space group). This quantitative analysis refers to crystallography data from the crystallography open database with card numbers (COD: 00-043-0002) for $CoFe_2O_4$ phase.

Phase formation, changes in lattice parameters, crystallite size, lattice strain, and cationic distribution of Zn substitution results into the cobalt ferrite lattice are based on refinement of X-ray diffraction patterns of $Co_{1-x}ZnxFe_2O_4$ samples with variations in composition (x = 0-1) for all samples shown in Table 2.

Table 2. Value of the structure parameters, fit criteria (Rwp), goodness of fit (χ^2) and the phase mass fraction formed in the $Co_{1-x}Zn_xFe_2O_4$ sample with variations in composition (x = 0-1).

Sample (x)	Phase	Lattice parameter (Å) a = b = c	V (Å^3)	ρ (g/cm^3)	Fraction wt%	R$_{wp}$ (%)	χ^2
0	$CoFe_2O_4$	8.3707(2)	586.52(5)	5.33	100	2.64	1.21
0.25	$Co_{0.75}Zn_{0.25}Fe_2O_4$	8.3957(3)	591.80(6)	5.29	100	2.70	1.91
0.5	$Co_{0.5}Zn_{0.5}Fe_2O_4$	8.4160(3)	596.11(7)	5.26	100	2.95	1.21
0.75	$Co_{0.25}Zn_{0.75}Fe_2O_4$	8.3971(2)	592.10(5)	5.28	100	2.83	1.19
1	$ZnFe_2O_4$	8.3729(5)	586.99(1)	5.05	100	2.69	1.29

The results of refinement of X-ray diffraction patterns in Figure 3 and Table 2 have very good fitting quality according to fit criteria (R$_{wp}$) and goodness of fit (χ^2) very good [19]. The Rwp statistical parameter is the weight ratio of the difference between the observation pattern and XRD pattern calculation where the best value is <10%, while the statistical parameter χ^2 (*chi-squared*) is the comparison ratio of the XRD pattern of calculation and expectation calculations where the best value is $1 < \chi^2 < 1.3$.

The crystal size and lattice strain were calculated based on the Williamson-Hall formula, which is the curve between sin θ as axis and β cos θ parameters as ordinate for some of the highest peaks of the XRD pattern. The Williamson-Hall formula is defined as (1) [20]:

$$\beta \cos\theta = k\frac{\lambda}{D} + 3\varepsilon \sin\theta \qquad (1)$$

With k being the scherrer (value 0.9), λ is the X-ray wavelength, θ is the Braggs diffraction angle, D is the crystalite size, β is the width at the maximum peak (FWHM in radians), and ε is the lattice strain. The β cos θ versus sin θ curve is calculated for the five highest peaks of the XRD pattern of the $Co_{1-x}Zn_xFe_2O_4$ sample with variations in composition (x = 0-1) as shown in Figure 4 (a-e). This data was analyzed by a linear function approach, so that both the crystallite size and the lattice strain were obtained from the ordinate interception and the slope of the curve as a linear function. The results of the calculation of both crystal size and lattice strain are shown in Figure 4 (f-j) for all samples.

The results of this refinement are also supported by observations of particle surface morphology for the single phase using SEM as shown in Figure 4 (f-j). In Figure 4 (f-j) shows that the particle morphology for all samples has very good and uniform particle homogeneity on all sample surfaces with cubic particle shapes with particle sizes varying from 100 nm to 500 nm. In general, the results of single phase characteristics of these polycrystalline samples according to SEM photo observations are homogeneity and uniform particle shape for $CoFe_2O_4$ phases across the sample surface.
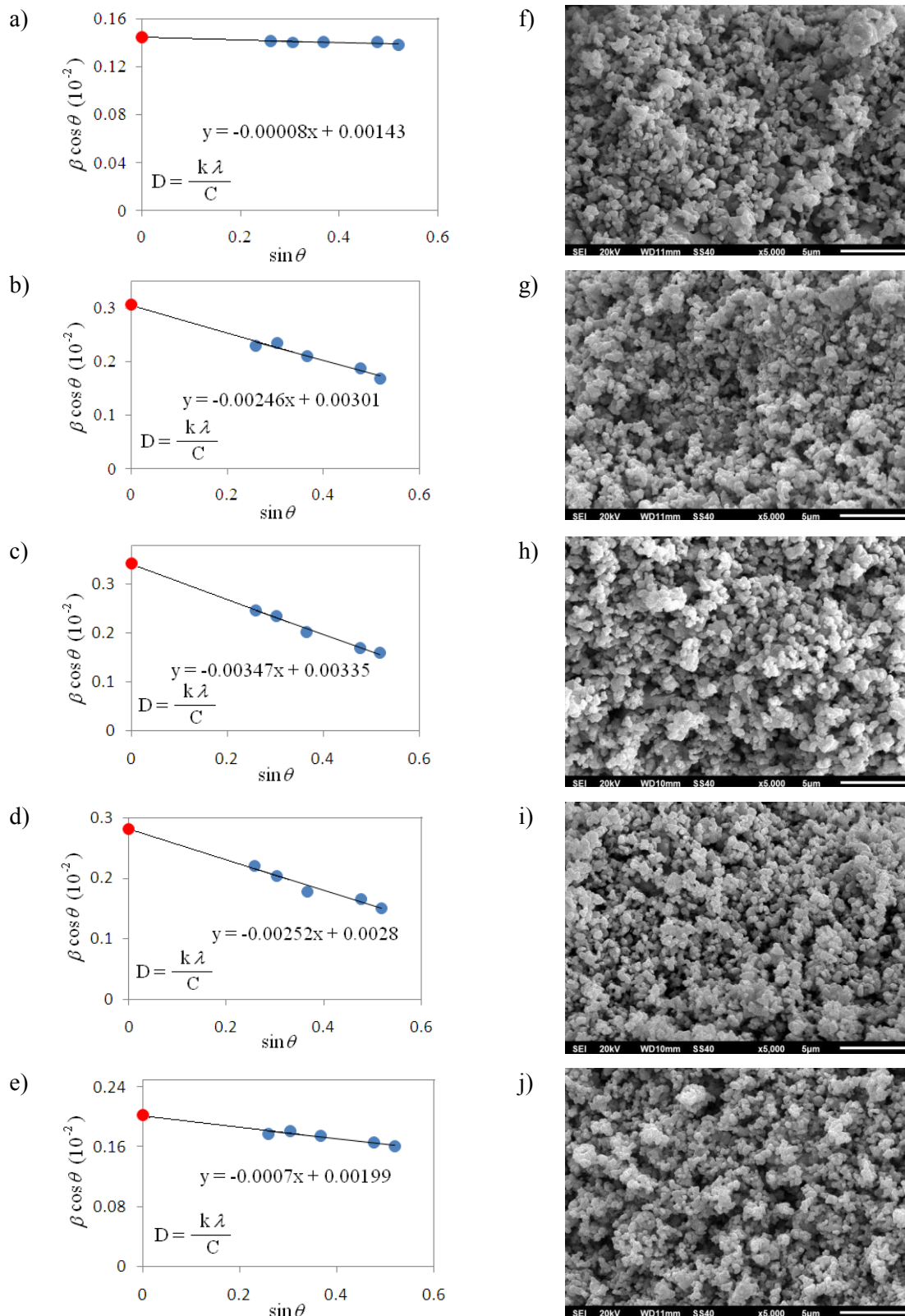
Figure 4. The results of the calculation of the crystallite size of the Williamson-Hall method and particle morphology $Co_{1-x}Zn_xFe_2O_4$ observed using SEM for samples (a) and (f) x = 0; (b) and (g) x = 0.25; (c) and (h) x = 0.5; (d) and (i) x = 0.75; (e) and (j) x = 1.

An interesting discussion found that the average crystallite size of $Co_{1-x}Zn_xFe_2O_4$ samples with variations in composition (x = 0-1) changed as a function of composition while the particle size distribution was almost constant for all samples (100-500 nm). Changes in the size of this crystallite to particle size that is almost constant are closely related to the magnetic anisotropy characteristics of these magnetic samples. Crystallite size for each composition x = 0, x = 0.25, x = 0.5, x = 0.75, and x = 1 are ± 97 nm, ± 46 nm, ± 41 nm, ± 49 nm, and ± 70 nm. The smallest crystallite size was found at the composition of x = 0.5 at D = ± 41 nm (D = ± 97 nm for x = 0) which is thought to have the greatest magnetocrystalline anisotropy because it is possible to decrease the domain wall area in each particle.
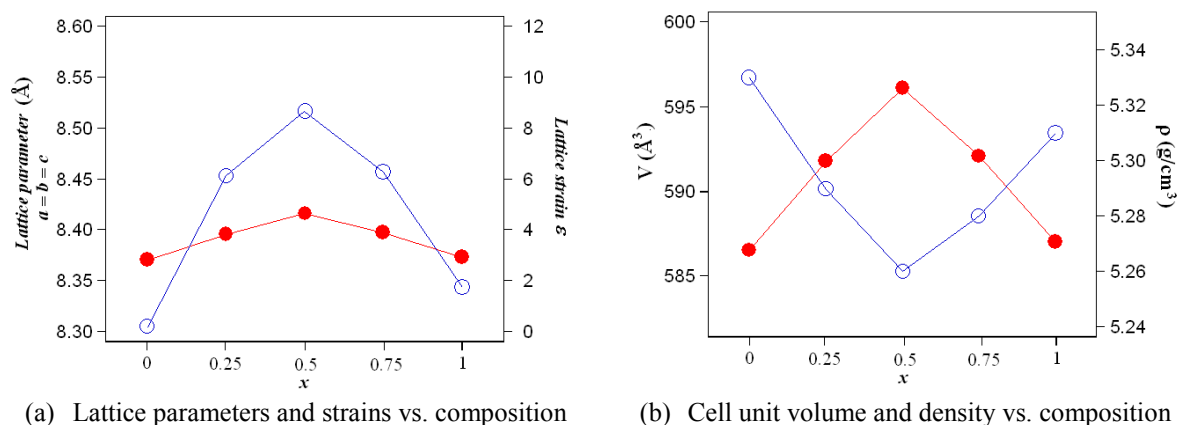

(a) Lattice parameters and strains vs. composition   (b) Cell unit volume and density vs. composition

Figure 5. Cell unit volume and atomic density as a function of composition

Based on the results of refinement of the X-ray diffraction pattern of $Co_{1-x}Zn_xFe_2O_4$ samples with variations in composition (x = 0-1), all samples have a single phase cobalt ferrite structure. Whereas the lattice parameters, cell unit volume, and atomic density change as a function of the composition of x as shown in Figure 5. In Figure 5 (a) it is shown that the highest lattice and strain parameters are found in the composition x = 0.5. Similarly, the volume of the largest cell unit and the smallest atomic density obtained at the composition of x = 0.5. This is because the radius of the Zn ion (r = 1.25 Å) is greater than the radius of Co ion (r = 1.16 Å), resulting in an increase in lattice parameters for all three crystallographic axes. This increase in lattice parameters causes the lattice strain especially in the grain boundary area and the cell unit volume increases. But the number of atoms in one cell unit remains while the volume of the cell unit increases, so that the atomic density gets smaller. However both lattice parameters, cell unit volume, and atomic density change as a function of composition x, spinel ferrite structure with cubic crystal symmetry (Fd-3m space group) can still be maintained.

The interesting thing to understand is that all samples have a single phase with the same structure, although the composition is different as illustrated in Figure 6. At the composition x = 0.25; 0.5; and 0.75, which means there are 25%, 50%, and 75%, respectively, have succeeded in replacing part of Co atoms which are expected to have an impact on other properties, especially on microwave absorption. In this case, it is necessary to analyze the cationic distribution by reflecting the atomic occupancy factor at the site of the Co atom which has been substituted with the Zn atom.
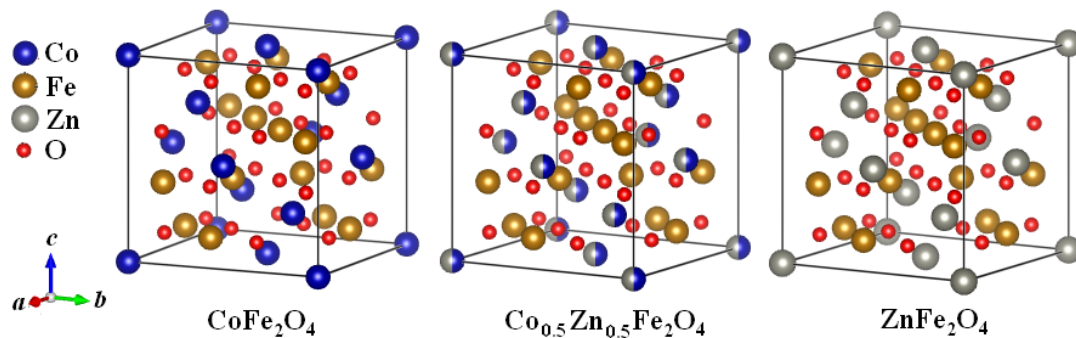
Figure 6. Illustration of $Co_{1-x}Zn_xFe_2O_4$ spinel ferrite structure with cubic crystal symmetry (Fd-3m space group)

The structure of $Co_{1-x}Zn_xFe_2O_4$ is a spinel ferrite structure with cubic crystal symmetry (Fd-3m space group). The position of the Co atom occupies the Wyckoff position at site 8a, the Fe atom occupies the Wyckoff position at site 16d, and atom O occupies the Wyckoff position at site 32e. One unit of cells $Co_{1-x}Zn_xFe_2O_4$ is formed by 56 atoms with 32 oxygen anions distributed in a closed cubic structure, and 24 cations consisting of 8 Co atoms on tetrahedral sites and 16 Fe atoms on octahedral sites [16]. Whereas the Zn atom will occupy part of the Wyckoff position of the Co atom at site 8a. Analysis of Co-O-Fe bond length and cationic distribution of refinement results are shown in Table 3.

Table 3. Cationic distribution is calculated based on the results of XRD data refinement

x	Site	Point symmetry	Bond length (Å)		Cationic distribution		
			Co – O	Fe – O	Co	Zn	Composition
0	8a	-43m	4.2275(12)	1.8377(3)	1.00 (100 at.%)	-	$CoFe_2O_4$
0.25	8a	-43m	4.2401(17)	1.8432(5)	0.76 (75.81 at.%)	0.24 (24.19 at.%)	$Co_{0.76}Zn_{0.24}Fe_2O_4$
0.5	8a	-43m	4.2507(14)	1.8478(4)	0.44 (44.20 at.%)	0.56 (55.80 at.%)	$Co_{0.44}Zn_{0.56}Fe_2O_4$
0.75	8a	-43m	4.2409(15)	1.8435(4)	0.25 (24.90 at.%)	0.75 (75.10 at.%)	$Co_{0.56}Zn_{0.75}Fe_2O_4$
1	8a	-43m	4.2286(18)	1.8381(5)	-	1.00 (100 at.%)	$ZnFe_2O_4$

Magnetic properties will be seen from changes in magnetic exchange interactions (Co-O-Fe) through the approach of calculating the bond distance between the atoms. Table 3 shows that the bonding distance of the nearest Co-O-Fe was found at the composition x = 0, meaning that the composition formed based on the cationic distribution analysis of $CoFe_2O_4$ has the best ferromagnetic properties and the farthest boundary found at composition x = 0.5, and based on the cationic distribution analysis has composition of $Co_{0.44}Zn_{0.56}Fe_2O_4$ and has the lowest ferromagnetic properties. Besides that, it is also obtained that the composition produced from this experiment approaches the desired composition of stoichiometry.

4. Conclusion

Synthesis of $Co_{1-x}Zn_xFe_2O_4$ with variations in composition (x = 0-1) has been successfully carried out as one of the candidates for microwave absorbing material using solid reaction method through mechanical deformation techniques. The refinement results from the X-ray diffraction pattern of the $Co_{1-x}Zn_xFe_2O_4$ sample indicate that the sample has a single phase for all x compositions. Particle morphology for all compositions x has good and uniform particle homogeneity on all sample surfaces with cubic particle shape and particle size around 100-500 nm. Lattice parameters, cell unit volume, atomic density, lattice strain and crystalite size change as a function of composition x. The highest

lattice parameters and strains were found in the composition x = 0.5. Similarly, the volume of the largest cell unit and the smallest atomic density obtained at the composition of x = 0.5. This is because the radius of the Zn^{2+} ion (r = 1.25 Å) is greater than the radius of Co^{2+} ion (r = 1.16 Å), resulting in increased lattice parameters for all three crystallographic axes. This increase in lattice parameters causes the lattice strain especially in the grain boundary area and the cell unit volume increases. But the number of atoms in one cell unit remains while the volume of the cell unit increases, so that the atomic density gets smaller. It was concluded that the lattice parameters, cell unit volume, and atomic density changed as a function of the composition of x, the spinel ferrite structure with cubic crystal symmetry (Fd-3m space group) could still be maintained.

Acknowledgement

References

[1]   Eswaraiah V, Venkataraman S, Sundara R 2011 Functionalized Graphene–PVDF Foam Composites for EMI Shielding *Macromol. Mater. Eng* **296** 1-5.

[2]   Kumar M, Vibha R, Gupta, and Sanjeeb K R 2014 Microwave Dielectric Properties of $Ni_{0.2}Cu_xZn_{0.8-x}Fe_2O_4$ for Application in Antenna *Progress In Electromagnetics Research B* **57** 157-175

[3]   Chakraborty H 2013 *Electromagnetic Interference Reflectivity of Nanostructured Manganese Ferrite Reinforced Polypyrrole Composites* **14**(6) 295–298.

[4]   Sameer D and Gagan D A 2014 Review on Effect of Electric Permittivity and Magnetic Permeability over Microwave Absorbing Materials at Low Frequencies *International Journal of Engineering and Advanced Technology* **3** 12-19.

[5]   Wisnu A A and Azwar M 2012 Structural and Absorption Characteristics of Mn-Ti Substituted Ba-Sr Hexaferrite Synthesized by Mechanical Alloying Route J*ournal of Basic and Applied Scientific Research* **2** (8) 7826-7834

[6]   Kiani E, Rozatian A S H and Yousefi M H 2014 Structural, magnetic and microwave absorption properties of $SrFe1_{2–2x}(Mn_{0.5}Cd_{0.5}Zr)_xO_{19}$ ferrite *J. Magn. Magn. Mater*. **361** 25-29

[7]   Bi-yu C, Ding C, Zhi-tao K and Ying-zhe Z 2015 Preparation and microwave properties of Ni-Co nanoferrites *Journal of Alloyas and Compounds* **618** 222 – 226.

[8]   Malhotra S, Chitkara M and Sandhu I S 2015 Microwave Absorption Study of Nano Synthesized Strontium Ferrite Particles in X *Band International Journal of Signal Processing, Image Processing and Pattern Recognition* **8**(10) 115–120.

[9]   Rafeekali K, Maheen M and Mohammed E M 2015 Influence of Rare Earth (Tb [3+]) on Electrical and Magnetic Studies of Nickel ferrite Nanoparticles *IOSR Journal of Applied Physics* **7**(3) 21–25. http://doi.org/10.9790/4861-07332125

[10]   Sonia M M L, Blessi S and Pauline S 2014 Role of Lathanum Substitution on the Structural and Magnetic Properties *International Journal of Advance Research In Science And Engineering* **8354**(3) 360–367.

[11]   Teber A, Cik K, Yilmaz T, Eraslan B, Uysal D, Surucu G, Baykal A H and Bansal R 2017 Manganese and Zinc Spinel Ferrites Blended with Multi-Walled Carbon Nanotubes as Microwave Absorbing Materials *Aerospace* **4**(2) 1-18 doi:10.3390

[12]   Tripathi K C, Abbas S M, Alegaonkar P S and Sharma R B 2015 Microwave Absorption Properties of Ni-Zn Ferrite Nano-Particle based Nano Composite *International Journal of Advanced Research in Science, Engineering and Technology* **2**(2) 463–468.

[13]   Xuan T A C, Bach N T, Le T H N, Manh H D, Phuc X N and Dao N H N 2016 Microwave absorbing properties of iron nanoparticles prepared by ball-milling *Journal of Electronic Materials* **45** 2311 – 2315.

[14]   Yarilyn C M, Oscar P P and Oswald N C U 2013 *Effect of high energy ball milling time on structural and magnetic properties of nanocrystalline cobalt ferrite powders Journal of Magnetism and Magnetic Materials* **341** 17 -24.

[15]   Mullai R U, Pradeep P P and Chandrasekaran G 2012 Synthesis And Characterization of Lanthanum Doped Mg-Zn Ferrite Nanoparticles Prepared by SOL-GEL Method *International Journal of Recent Trends in Science And Technology* **5**(2) 78-85.

[16]   Gafton E V, Bulai G, Caltun O F, Cervera S, Ace S, Trassinelli M, Steydli S and Vernhet D 2016 Structural and magnetic properties of zinc ferrite thin films irradiated by 90 keV neon ions *Applied Surface Science* Appl. Surf. Sci. **379** 171–178

[17]   Toby B H and EXPGUI 2001 A Graphical User Interface for GSAS *J. Appl. Crystallogr.* **34** 210–221

[18]   Hajalilou A, Saiful A M and Kamyar S 2016 A comparative study of differet concentrations of pure Zn powder effects on synthesis, structure, magnetic and microwaveabsorbing properties in mechanically-alloyed Ni-Zn ferrite *Journal of Physics and Chemistry of Solids* **96-97** 49 – 59

[19]   Kumar S, Supriya S, Pradhan L K, Manoranjan K 2017 Effect of microstructure on electrical properties of Li and Cr substituted nickel oxide *J. Mater. Sci.: Mater. Electron* **28** 16679

[20]   Tadjarodi A, Rahimi R, Imani M, Kerdari H and Rabbani M 2012 Synthesis, characterization and microwave absorbing properties of the novel ferrite nanocomposites *Journal of Alloys and Compounds* **542** 43 – 50